Air-Lift Bioreactors for Algal Growth on Flue Gas: Mathematical Modeling and Pilot-Plant Studies

Gordana Vunjak-Novakovic,*,† Yoojeong Kim,‡ Xiaoxi Wu,‡ Isaac Berzin,‡ and José C. Merchuk§

Massachusetts Institute of Technology, Cambridge, Massachusetts 02139, GreenFuel Corporation, Cambridge, Massachusetts 02139, and Ben-Gurion University of the Negev, Beer-Sheva, Israel

Air-lift reactors (ALRs) have great potential for industrial bioprocesses, because of the low level and homogeneous distribution of hydrodynamic shear. One growing field of application is the flue-gas treatment using algae for the absorption of CO_2. In this paper, we discuss the requirements for photosynthetic biomass growth in an ALR. The effects of the operating variables are analyzed using a mathematical model [Wu, X.; Merchuk, J. C. Simulation of Algae Growth in a Bench Scale Internal Loop Airlift Reactor. *Chem. Eng. Sci.* **2004**, *59* (14), 2899] that accounts for the effects of ALR geometry, fluid flow, and illumination on the biomass growth. On the basis of the ALR principles and the specific requirements of photosynthetic processes, we developed a "triangular" ALR configuration that is particularly suitable for algal growth. We describe the design and operation of this novel bioreactor and present the first series of experimental data obtained for two different algal species in a pilot-scale unit supplied with flue gases from a small power plant. The measured removal efficiency of CO_2 was significant ($82.3 \pm 12.5\%$ on sunny days and $50.1 \pm 6.5\%$ on cloudy days) and consistent with the increase in the algal biomass.

Introduction

The air-lift reactor (ALR) is a type of pneumatic contacting device in which fluid circulation takes place in a defined cyclic pattern through channels built specifically for this purpose. ALRs are considered to have vast potential in industrial bioprocesses, because of the low level and homogeneous distribution of hydrodynamic shear. However, not many examples are known of large-scale applications. There are two general types of biological processes, both related to ecoconservation, that are inherently large-scale and can take advantage of the ALR. For one class of processes—wastewater treatment—several configurations have been proposed.[2−8] The second class of processes is a relatively novel application of the ALR to the flue-gas treatment using algae for the absorption of CO_2 and abatement of NOx. The interest of NASA for controlled algal-based ecological life support systems in space has fueled the research of algal reactors and optimization for biomass production in the 1980s and 1990s.[9]

The importance of mixing in the proper operation of a chemical reactor has been studied extensively because of its relevance to yield and stability. A proper solution is likely to involve a combination of macromixing of the bioreactor contents (controlled by proper sizing of the vessel and driven by aeration) and micromixing at the molecular level. In the case of biochemical reactions, the situation becomes more complex, because of the possible effects of hydrodynamic shear on the kinetics of cell division or product synthesis.[10] Additional effects may result from spatial gradients within the system (in particular, in large-scale systems), such as those resulting from nonhomogeneous distribution of light in the case of photochemical reactions.

Clearly, a deeper knowledge of the bioreactor fluid dynamics is needed for their rational design and optimization. The conventional description of flow by residence time distribution, customary in chemical reactors, may not provide sufficient information for an accurate description of photobioreactions. Fluid elements that spend the same time in the reactor but stay in different light-intensity regions will have different kinetic behavior. To evaluate this effect and to model the process, knowledge on fluid trajectories is necessary. Only a model that takes into account this point will be able to predict correctly the effects of scale-up on the performance of the reactor.

A schematic presentation of an ALR with concentric tubes is shown in Figure 1. Other configurations, such as external loops or split vessels, have essentially the same regions: a riser (draft tube in Figure 1), a gas separator, and a downcomer (annulus in Figure 1). In the riser, gas injection produces a highly turbulent region with high gas holdup. In the downcomer, the liquid returns to the bottom after separating from the gas bubbles that disengage in the gas separator. A fraction of gas may eventually be entrapped in the downcomer, depending on the ALR geometry and operating conditions: The gas holdup, however, remains lower than that in the riser, and the difference in the gas holdups between the two regions produces the difference in the apparent fluid density that drives the liquid circulation. In terms of gas−liquid flow configurations, in the riser and separator we will find bubbly or bubbly turbulent flow. In the downcomer, the liquid will

* To whom correspondence should be addressed. Tel.: (617) 452-2593. Fax: (617) 258-8827. E-mail: Gordana@mit.edu.
† Massachusetts Institute of Technology.
‡ GreenFuel Corp.
§ Ben-Gurion University of the Negev.

10.1021/ie049099z CCC: $30.25
Published on Web 06/28/2005

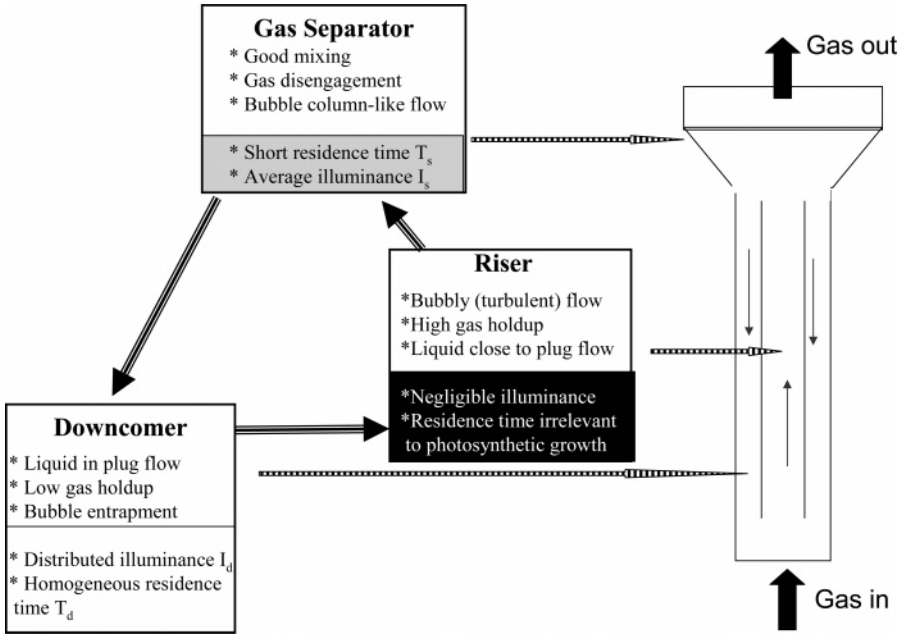

Figure 1. Schematic presentation of an ALR for culture of photosynthetic cells. The difference in the apparent fluid densities between the riser and downcomer provides the driving force for liquid circulation. It is assumed that (i) the riser is completely dark, (ii) the gas separator provides homogeneous and constant illumination, and (iii) there is an exponential decrease profile of the light intensity in the downcomer.

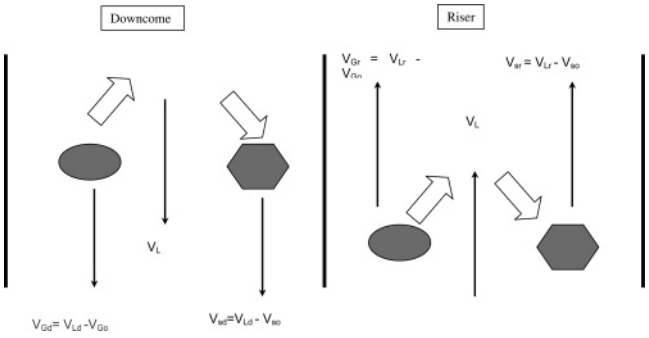

Figure 2. Liquid, gas, and solid velocities in a three-phase ALR. Arrows indicate the mass transfer from the gas bubbles (elliptical) to the liquid and from the liquid to the particles (hexagonal). Black arrows indicate the direction of the velocity vector.

usually show a near-plug-flow behavior, as long as the tubes are vertical.[11]

If solids (e.g., suspended living cells) are present in the system, they will exert an influence on the flow, with strong dependence on the density difference between the solid and liquid phases.[12] The analysis can be simplified by assuming that the velocity of the solid particles relative to the liquid is the free-fall velocity and that the velocity of the bubbles relative to the liquid is the free-rise velocity. In this case, the mass-transfer rates between the liquid phase and either particles or bubbles are comparable for the riser and downcomer (Figure 2). This assumption facilitates the prediction of the solid−liquid mass-transfer rates because available correlations for liquid-particle mass transfer become applicable. In the case of gas−liquid mass transfer, the situation is complicated by different surface areas for gas−liquid mass transfer in the riser, gas separator, and downcomer.

In this paper, we first discuss the specific requirements for photosynthetic biomass growth in an ALR. The effects of the operating variables are analyzed using a mathematical model of Wu and Merchuk[1] that accounts for the effects of both fluid flow and illumination on photosynthetic biomass growth. On the basis of the available ALR theory and the specific requirements of biological processes involving photosynthetic organisms, we developed a "triangular" ALR configuration that is particularly suitable for algal growth on flue gases. We describe the design and operation of this novel bioreactor and present the first series of experimental data obtained for two different algal spieces in a pilot-scale unit operated outside and fed by a flue gas.

Photosynthetic Biomass Growth in an ALR

Like many plants, algae convert CO_2 (carbon dioxide) to organic material in photosynthetic reactions. Electrons for this reduction reaction ultimately come from water, which is converted to oxygen and protons. The energy for this process is provided by light, which is absorbed by pigments (primarily chlorophylls and carotenoids). Photosynthesis is a two-stage process (Figure 3). Phase I ("light reactions") is light-dependent and requires the energy of light to make energy carrier molecules that are used in the second process. Phase II ("dark reactions") is light-independent and occurs when the products of phase I are used to form C−C covalent bonds of carbohydrates. Recent evidence supports the importance of light and dark cycles[13] and suggests that a major enzyme of the "dark reactions" is indirectly stimulated by light; thus, the term "dark reaction" is somewhat of a misnomer.

In an ALR, light flux decreases exponentially with the distance from the irradiated surface. The algae near the irradiation source are thus exposed to a high photon density, which enhances the growth rate, as compared to the cells at the center of the ALR tube, which receive less light as a result of shading and grow more slowly. However, excessive light can damage protein D1 in photosystem II (photoinhibition) and decrease the growth rate because of the reduction in the number of active

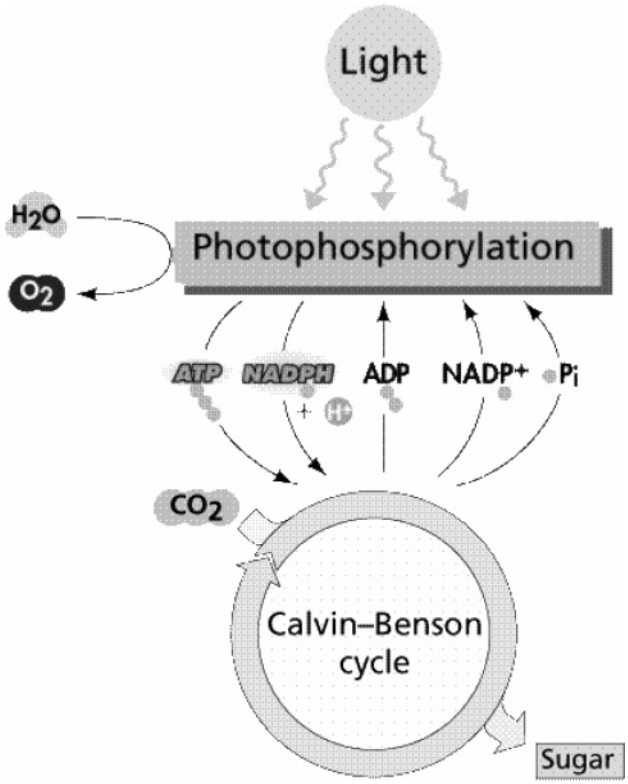

Figure 3. Overview of the two phases of the photosynthesis process. Light energy is absorbed in light reactions of phase I, stored in the form of ATP and NADPH, and utilized for biomass production in dark reactions of phase II. In light reactions, water is split and oxygen evolves. In dark reactions, carbon dioxide is incorporated into the biomass via a Calvin−Benson cycle.

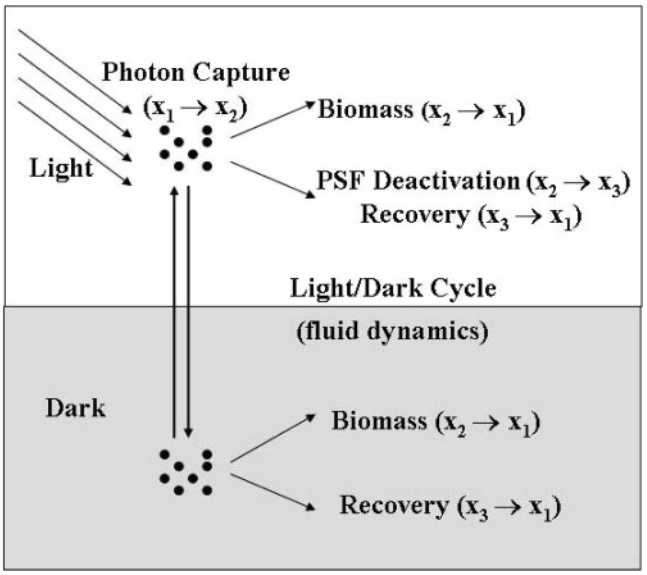

Figure 4. Schematic representation of the interaction of illumination and the fluid dynamics in a photosynthetic cell culture. The volume is divided into two regions, one dark and one illuminated. Photons are captured by the cells in the illuminated region by open PSFs (state x_1), and both photosynthesis (transfer to state x_2) and PSF deactivation (transfer to state x_3) can take place. The cells are cyclically transported to the dark zone, where PSF recovery takes place. Reprinted with permission from ref 18. Copyright 1998 Wiley.

"photon traps".[14,15] Therefore, the growth rate can be influenced not only by the intensity but also by the history of the illumination,[16] and a periodical change in illumination can enhance growth.[17]

Previous work[18] suggested a general approach that integrates the fluid dynamics of an ALR with the mathematical description of photosynthesis and accounts for both the stimulatory and inhibition effects of light. The model is suitable for analyzing the growth phase and does not consider secondary metabolite production. The mathematical representation of the photosynthetic growth in an alternating light−dark regime by Merchuk and colleagues[18] is based on the three-state model of a photosynthetic factory (PSF) developed earlier by Eilers and Peters.[19] The model supports the notion that the utilization of light−dark cycles may enhance the photosynthetic growth, which in turn implies that ordered mixing can be utilized to enhance growth. The model can predict the effects of insufficient or excessive illumination and account for the effects of mixing on the biomass growth. The kinetics of photosynthesis can thus be modeled under the conditions of photoinhibition in one region of the reactor (because of too much light) and photolimitation in another (because of little or no light), a situation frequently encountered in ALRs.

The concept of the PSF[19] that forms the biological basis of the model developed by Wu and Merchuk[1,11,20,21] involves three states: the resting state (x_1), the activated state (x_2), and the inhibited state (x_3). The PSF in the resting or open state can be stimulated and transferred to the activated state when it captures a photon. The PSFs in the activated state can either receive another photon and become inhibited or pass the gained energy to acceptors to start photosynthesis and then return to the open state. The inhibited PSF, meanwhile, can recover by returning to the open state.

Figure 4 shows a simplified scheme that was used by Wu and Merchuk[1] to show the interaction of fluid dynamics and photosynthesis. It consists of two zones, one dark and one of a certain constant illuminance. The figure shows schematically which of the steps of the PSF model (see the description above) take place in each region.

In an actual photobioreactor, the situation is more complex. Let us take the example of an ALR with concentric tubes. The region of the ALR riser can be regarded as the dark zone and the rest of the ALR volume as the light zone with variable illuminance (Figure 4). In the riser (dark zone), the cell kinetics does not depend on the illuminance, and hence the flow pattern in this region has no influence on the light utilization. In the gas separator, the flow rates are rather high, such that perfect mixing can be assumed.[22,23] Because of the short residence times, the light history of the cells within the separator can be approximated as one of constant illuminance. In the downcomer, the cells are illuminated and the residence times are relatively long, such that both the detailed flow pattern and the illumination history are of high interest. Because of the relatively low gas flow rates, the regimes of interest for algal growth are homogeneous bubbling flow in the riser and plug flow in the downcomer with none or minimal gas recirculation.[11]

For model development, the downcomer was divided into several radial regions representing light zones with a constant level of illuminance. The fraction of the cells in each light zone was calculated based on the assumption that algal cells are homogeneously distributed in the downcomer. For each cycle, the concentration value

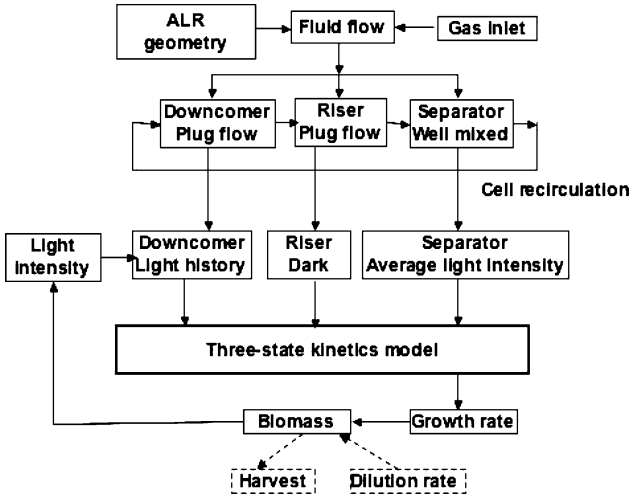

Figure 5. Mathematical model of algal growth in an ALR. Dashed lines and boxes are for the continuous mode of operation.

of the biomass was adjusted to account for the growth, and this value is used for the next cycle. The differential equations describing the kinetics of biomass growth are as follows:

$$dx_1/dt = -\alpha I x_1 + \gamma x_2 + \delta x_3$$

$$dx_2/dt = \alpha I x_1 - \gamma x_2 - \beta I x_2$$

$$x_1 + x_2 + x_3 = 1$$

$$\mu = k\gamma x_2 - \mathrm{Me}$$

where α, β, γ, and k are kinetic constants and Me is the maintenance term.

The algorithm used to solve the differential equations and obtain predictions for cell concentrations as a function of the operating variables is depicted in Figure 5. For details on the model development and solution, see refs 1, 11, and 20.

Model Predictions for Algal Growth in a Concentric-Tube ALR under Continuous-Flow Conditions

In the present study, the model was solved for the case of continuous operation (Figure 5). A batch operation involves an increase in the cell concentration (i.e., amount of biomass) until the growth becomes limited by either the available nutrients or (more common) the light input, and the cell concentration saturates at a constant level. In a continuous mode, a fraction of the biomass is harvested and the content of the bioreactor is diluted at timed intervals. The conditions thus correspond to a series of batchwise operating cycles. If the dilution factor is small and the biomass is harvested frequently, the operating conditions approach pseudo-steady-state operation.

Model simulations for continuous operation were made with the same general assumptions as those explained previously for the batch operation. For a given dilution rate, the conditions of pseudo-steady-state operation were defined, and the biomass concentration was calculated. The biomass output and ground productivity were then calculated. Some interesting results of these calculations, showing the effects of key variables on biomass growth, are presented in Figure 6. The baseline set of conditions for model simulations was

superficial gas velocity (riser based)	$J_G = 0.334$ cm/s
light intensity at the reactor wall	$I_0 = 250$ μE/m^2·s
column height	$H_T = 1.0$ m
ratio of cross-sectional areas of the riser and downcomer	$A_r/A_d = 0.8$

In each case, one of the above parameters was varied within a range of interest for an algal culture in a concentric-tube ALR.

The volumetric output of the biomass (in millions of cells produced per milliliter of bioreactor volume per hour), a measure of the bioreactor productivity, decreases with an increase in the bioreactor diameter, at a rate that further depends on the A_r/A_d ratio (Figure 6A). An increase in the bioreactor diameter to 1 m reduced the volumetric productivity to very low levels, at all A_r/A_d ratios studied (0.5, 1, and 1.46). At any column diameter (Dc), the productivity decreased as the A_r/A_d ratio increased, consistent with the fact that the fraction of the reactor volume that is dark increases with an increase in A_r/A_d. Taken together, these results are consistent with the fact that the decrease in the light input, associated with either an increase in Dc or the A_r/A_d ratio, results in photolimitation, which in turn decreases the production of the biomass.

The effect of the A_r/A_d ratio on the volumetric output of the biomass at baseline conditions is shown in Figure 6B (data points). The corresponding optimal dilution rates are shown in the same graph (line). The biomass productivity decreases with an increase of the A_r/A_d ratio, first slowly (at $A_r/A_d < 1$) and then more rapidly (at $A_r/A_d > 1$), such that the biomass production is effectively diminished at A_r/A_d approaching 1.5. This is consistent with the fact that an increase in the A_r/A_d ratio results in an increased fraction of the dark region in the bioreactor, at the expense of the illuminated regions.

At baseline conditions, the dilution rate can further affect the maximum cell concentration (X, 10^6 cells/mL), maximum output of biomass DX (10^6 cells/mL·h), and ground productivity of the biomass (10^9 cells/m^2 of ground surface area·h), as shown in Figure 6C. The ground productivity (Pg) is considered, as explained previously,[1,21] to account for the empty space that has to be left between bioreactors, either for maintenance or for adjustment of the illumination. In this simulation, the distance between each of the two bioreactors was 0.9 m, the same value as that previously used for algal cultivations. Overall, there appears to be an optimal rate of dilution for the maximum volumetric productivity, whereas the cell concentration decreases as expected with an increase in the dilution rate. Interestingly, the ground productivity was not very sensitive to the dilution rate in the range of conditions studied, but the maximum value of Pg was determined at the same dilution rate as the maximum of DX.

An increase in the bioreactor diameter under baseline conditions resulted in a decrease in the cell concentration and an associated decrease in the optimal dilution rate (Figure 6D). The ground productivity Pg passed through a maximum, suggesting that there is an optimal bioreactor diameter, approximately 0.5 m under the baseline conditions studied.

The predicted effects of light intensity PFD (photon flux density, μE/m^2·s) are shown in Figure 6E. An increase in the light intensity resulted in an initial

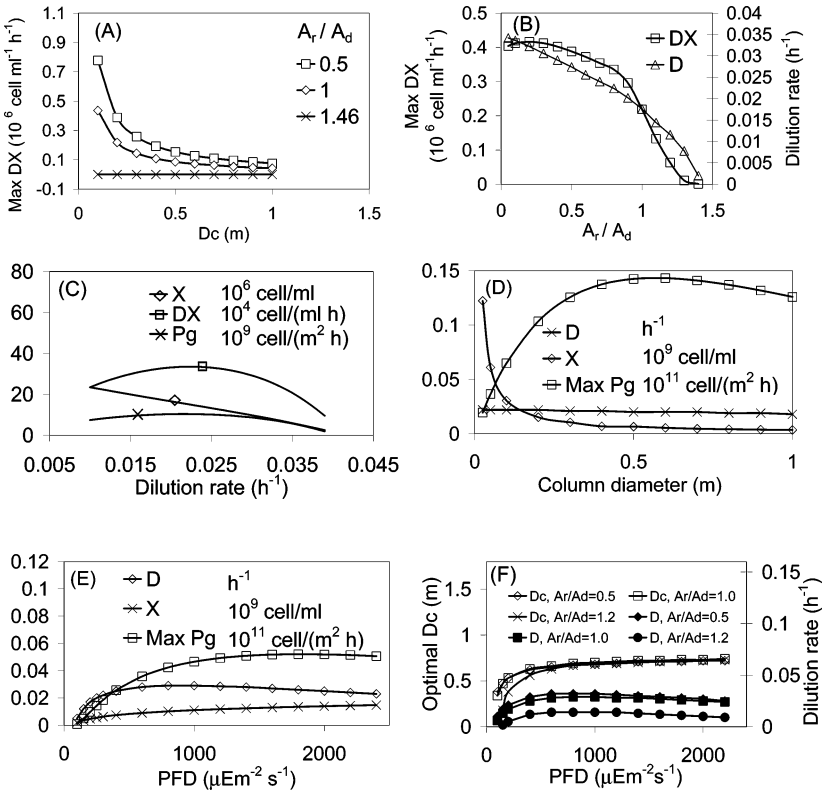

Figure 6. Simulation of a concentric-tube ALR operated in a continuous-flow mode. The parameters were maintained at baseline conditions (J_G = 0.334 cm/s, I_0 = 250 μE/m^2·s, H_T = 1.0 m, and A_r/A_d = 0.8) unless otherwise stated. (A) Effect of the ALR diameter Dc on the volumetric productivity DX of the biomass, at three different A_r/A_d ratios. (B) Effects of the A_r/A_d ratio on the DX and optimal dilution rate D. (C) Effects of the dilution rate D on the cell concentration X, volumetric biomass productivity DX, and ground productivity Pg. (D) Effects of Dc on the optimal dilution rate D, cell concentration X, and ground productivity Pg. (E) Effects of the illumination PFD on the optimal dilution rate D, cell concentration X, and ground productivity Pg. (F) Effects of PFD on the optimal Dc and dilution rate D, at three different A_r/A_d ratios.

increase in the cell concentration (consistent with photostimulation) followed by a decrease in the cell concentration (consistent with photoinhibition). The ground productivity increased with PFD but leveled off at a constant level at higher values of PFD.

For purposes of the initial system optimization, the simulations were performed at baseline conditions as the following series of steps:

1. For given PFD and Dc, find the optimal dilution rate for maximum Pg (Figure 6C).

2. Repeat step 1 for a series of Dc values (Figure 6D) and calculate the ground productivity.

3. Determine the optimal Dc.

4. Repeat steps 1−3 for a series of PFD values (Figure 6E).

5. Determine the light intensity and column diameter for an ALR operating at the maximum Pg. This last step is key for the design of ALR for algal growth.

The results of simulations are shown in Figure 6F. The optimal Dc and dilution rate are shown as a function of PFD, for a series of values of A_r/A_d, at baseline conditions (J_G = 0.334 cm/s; H_T = 1.0 m). For all values of A_r/A_d, the optimal column diameter increased slightly when PFD increased from 800 to 2200 μE/m^2·s, a range typical for an outdoor daytime illuminance. At the top of this range, Dc leveled off at a constant value, suggesting that the ratio between the illuminated and dark regions becomes controlling. Consistently, the A_r/A_d ratio had little effect on the optimal Dc at high PFD values. Also the wide range of PFD had little effect on the optimal dilution rate. However, larger A_r/A_d should be avoided because this will give a low growth rate and a less dense culture.

The simulations presented here are only qualitative in nature because they are based on extrapolations. Nevertheless, these simulations show that this model has the potential to be applied for ALR design and optimization according to a selected objective function.

Inclined-Tube ALR Configuration

The above description of mathematical modeling and simulations, and the way they integrate fluid dynamics and biokinetics, refers to the conventional vertical ALRs. The theory and findings from these studies were used as the basis for designing a new class of ALRs that utilize an inclined-tube configuration. Here we describe the design features of inclined-tube ALRs and report the experimental studies of algal growth on a flue gas in small-scale units operated under laboratory conditions and pilot-scale units operated on the roof of a power plant.

When gas is supplied from the bottom of an inclined tube, the gas bubble will travel the tube along the inner upper surface. This will renew the liquid layer of the upper surface, making it difficult for algae to adhere and thereby preventing fouling. Because this upper surface is usually arranged for light penetrating into the reactor, this self-cleaning feature can greatly reduce the maintenance requirement. Notably, we have not observed any signs of fouling after several months of continuous algal growth in inclined-tube bioreactors. We

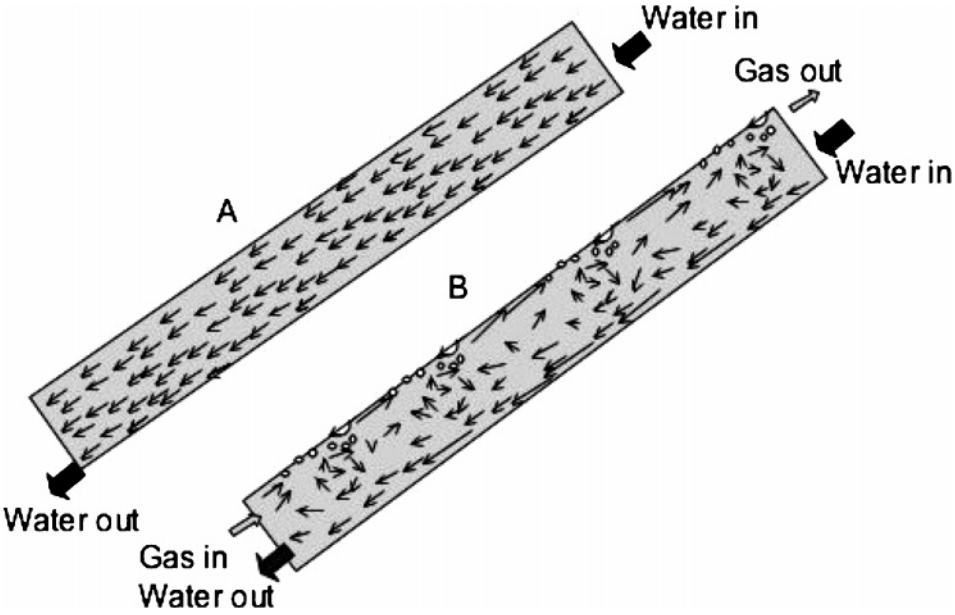

Figure 7. Visual observations of flow patterns in the inclined-tube ALR: (A) flow of liquid alone; (B) liquid−gas counterflow with bubbles introduced at the bottom of the tube.

Table 1. Selected Models for Airlift Fluid Dynamics and Mass Transfer[a]

source	gas−liquid system	gas−liquid−solid system	gas recirculation	V_L	ϵ_{Gr}	ϵ_{Gd}	ϵ_{Sr}	ϵ_{Sd}	ϵ_G	CFD
Heijnen et al.[28]	×	×	×	×					×	
van Benthum et al.[29]	×	×	×	×						
Garcia-Calvo et al.[3]		×		×	×		×	×		
Hwang and Lu[30]		×	×							
Freitas et al.[4]	×	×	×	×	×	×	×	×		
Mude and Van Den Akker[31]	×			×	×					×
Camarasa et al.[32]	×			×	×					
Camarasa et al.[33]	×			×	×					
Mousseau et al.[5]		×	×	×						
Saez et al.[34]	×			×	×	×	×			
Marques et al.[35]	×			×	×	×				
Cockx et al.[36]	×			×	×	×				×
Couvert et al.[6]	×			×	×	×				
Tobajas et al.[37]		×		×	×					
Camacho Rubio et al.[38]	×		×	×	×	×				
Sanders et al.[39]	×		×	×	×	×				
Shechter et al.[40]		×		×	×		×	×		
Orejas[41]				×	×					
Steiff et al.[42]	×		×	×	×	×				

[a] ×'s indicate elements that were taken into account in the model.

found this to be quite remarkable and most likely due to the dynamic hydrodynamic shear imposed by bubbling flow.

The above two features of the inclined tubes make them attractive for photobioreactor system applications. The first efforts in this area were directed toward the establishment of "flow pattern maps" via correlation of experimental data to predict the flow configurations for a given ALR geometry and gas and liquid flow rates.[24−26] Once the flow configuration is determined, one can estimate important characteristics such as the pressure drop, phase holdups, and heat/mass-transfer rates.

Generalization of this information and the ability to make extrapolations beyond the range of experimental data require a deeper insight into how flow configurations are generated and into the mechanisms of transition from one configuration to another. Models developed thus far include the correlations adapted from horizontal flow to inclined tubes and those able to predict the transitions between the flow configurations in inclined tubes (Table 1).[24,26] The later models are based on force balances for the liquid and gas phases, and they allow one to define the flow configuration and predict the gas holdup and pressure drop. However, none of the available models can predict the flow paths in the continuous liquid phase, which is the most important information for mathematical modeling of inclined-tube ALR for biomass growth.

We recently conducted flow studies in a two-dimensional inclined duct, representing one thin axial section of the inclined-tube ALR, using liquid tracer dyes. The flow rates of liquid (flowing downward) and gas (flowing upward) were independently controlled. The local velocities of the liquid and gas phases were estimated visually from the dye tracer experiments and are shown schematically in Figure 7. The flow of liquid alone was laminar in the whole ALR volume except for the calming section at the top of the inclined tube (Figure 7A). Introduction of even a small amount of gas caused a dramatic change in the flow pattern of liquid (Figure 7B). The gas was observed to creep along the upper wall as discrete bubbles, which coalesced after a certain

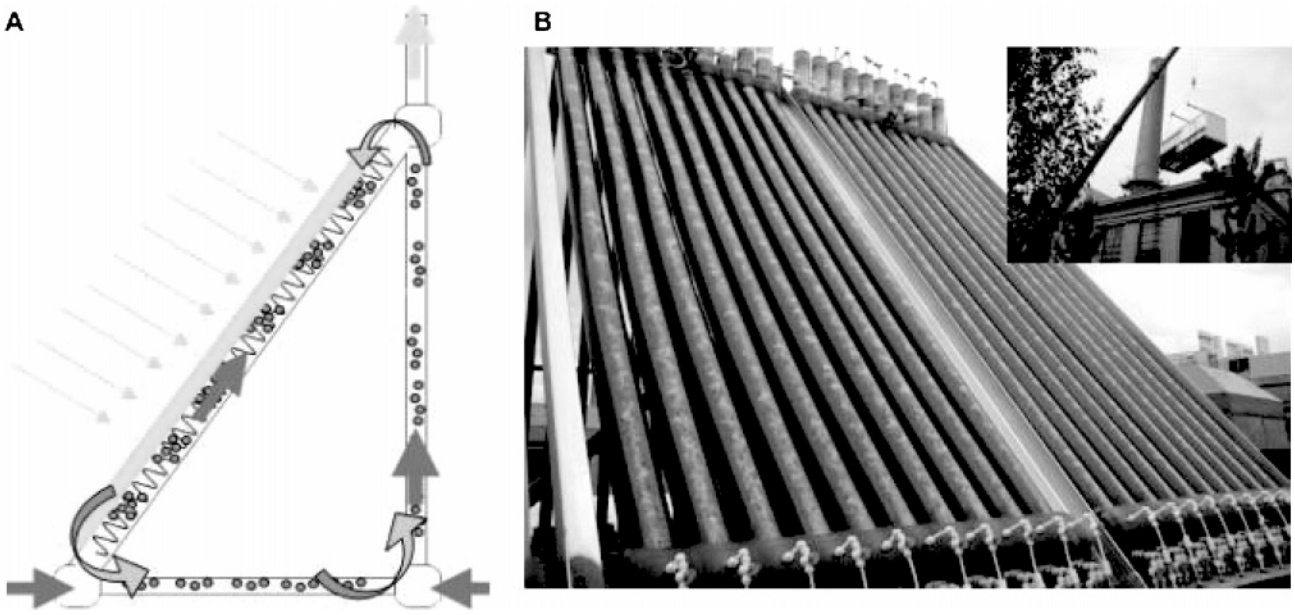

Figure 8. Inclined-tube ALR configuration: (A) schematic presentation of one ALR "triangle". Solid arrows indicate the direction of the gas flow, and open arrows indicate the direction of the liquid flow (B). An array of 30 ALRs, each with a volume of 30 L, with an algal culture grown on a flue gas. Inset: installation of the array of ALRs on the roof of MIT's Cogeneration Power Plant.

length into larger bubbles, generating a swirl that advances to the upper part of the device. In the bottom of the tube, very fast downward flow was established, balanced by a similar upward flow at the upper wall. These preliminary observations suggested that the presence of gas bubbles transformed liquid flow from laminar into turbulent and generated convective mixing in the liquid phase. Like in most other ALR configurations, the rate of liquid circulation is essentially determined by the gas flow rate.

To test the utility of the inclined-tube configuration for cultivation of unicellular photosynthetic algae, we designed and constructed a pilot-scale bioreactor shown in Figure 8. The particular application we are interested in is the flue gas treatment using algae. In this case, the nutrients for algal growth are provided by absorption of CO_2.

The schematic in Figure 8A describes the inclined-tube algal ALR. The working principle of this vessel is the same as that for a concentric-tube ALR, with a few differences. Most of the direct solar radiation enters through the hypotenuse, which is 3.3 m long, with a circular cross-sectional area. Thus, the cross section has an "intensive light" region, corresponding to that in the annular region of a concentric-tube ALR. The liquid flow rate through the prototype is controlled principally by the flow rate of the feed gas and can be adjusted to give a wide range (seconds to minutes) of retention time within each of the ALR regions. As the algae circulate through the inclined-tube segment, turbulence created by two gas spargers creates microtrajectories that carry the suspended cells back and forth between different light zones (i.e., closer to the illuminated surface or deeper into the liquid flow).

The desired capacity of flue gas purification is achieved by increasing the number of ALR "triangles" that are connected in parallel. Our second pilot-plant unit, shown with active algal cultures in Figure 8B, is a battery of 30 ALRs, each having the configuration shown in Figure 8A and a volume of 30 L. The system has been tested under the actual conditions, on the roof of the Cogeneration Power Plant at the Massachusetts Institute of Technology, Cambridge, MA. The inset shows the installation of the ALRs on the roof, in Spring 2004. The main component of the power plant is the ABBGT10A Combustion Turbine Generator set (ABB STAL AB, Finspång, Sweden). This includes the ABB EV (*EnVironmental*) combustor, which has a low level of NO_x emission. The flue gas contained approximately 20 ppm of NO_x and 8% CO_2 and was supplied at a flow rate of 600−800 mL/min per bioreactor vessel.

The feasibility of the algal culture with a flue gas at the MIT's Cogeneration Power Plant was demonstrated for two algal species and two different inclined-tube ALRs. Preliminary experiments were performed in a smaller-scale laboratory ALR that had a working volume of 7 L and no means of internal temperature control. Therefore, the laboratory ALR was enclosed in a wedge-shaped greenhouse with a triangular side view that resembled the shape of the reactor. It had an inclined window in front and two side windows, and the back was closed with a door. The greenhouse and the reactor were installed on the roof of the MIT power plant. The temperature inside the greenhouse was controlled by a thermostat that turned on a space heater or an air conditioner as needed.

For the setup in greenhouse, the flue gas was tapped from a pathway before the stack and delivered to the reactor by an oil-less diaphragm pump (DOA-701-AA, Gast Manufacturing Inc., Benton Harbor, MI). During turbine operation, water was injected into the combustion zone to reduce the thermal NO_x levels by cooling the flame. Therefore, the flue gas contained significant amounts of water. A water trap bottle was placed before the pump to capture condensed water accumulated in the delivery lines. The gas was introduced to the reactor by two spargers, and the flow rates were controlled using rotameters.

We tested two strains of green algae, *Dunaliella parva* (UTEX LB1983) and *Dunaliella tertiolecta* (UTEX LB999). The modified f/2 medium[27] was used. The composition of the modified f/2 medium was (per liter): 22 g of NaCl, 16 g of Aquarium Synthetic Sea Salt (Instant Ocean Aquarium Salt, Aquarium Systems, Inc.,

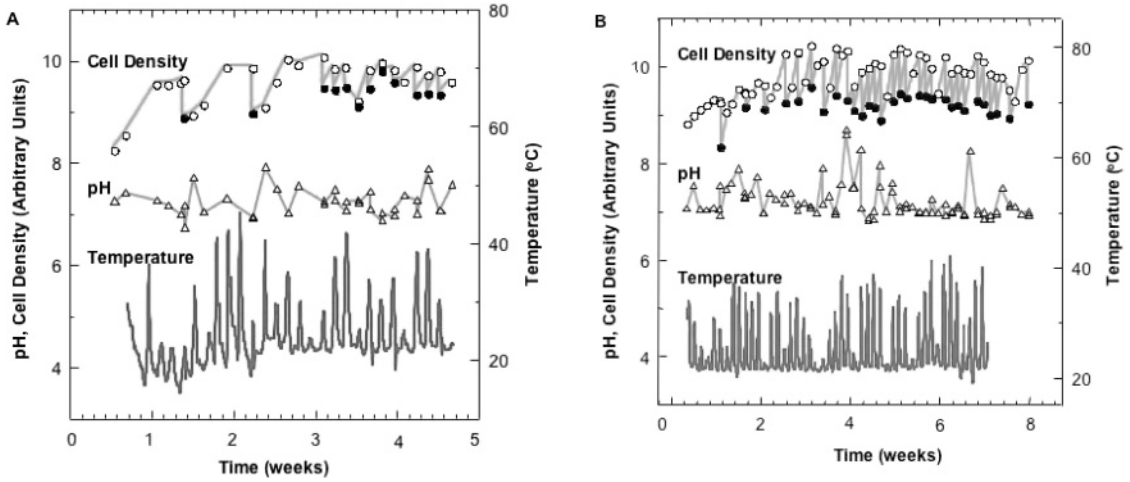

Figure 9. Algal growth on a flue gas in a pilot-plant unit at the Cogeneration Power Plant at MIT. (A) A 4-week culture of *D. parva*. The first two closed circles indicate the cell densities after harvesting 30% of the medium volume from the ALR and replacing it with a fresh medium. The rest of the closed circles are the results after 15% harvesting and replenishment. (B) An 8-week culture of *D. tertiolecta*. The closed circles represent the cell density after 30% harvesting. The bottom lines show the temperature of the reactor.

Mentor, OH), 425 mg of $NaNO_3$, 4.36 mg of EDTA·2Na, 3.15 mg of $FeCl_3 \cdot 6H_2O$, 180 μg of $MnCl_2 \cdot 4H_2O$, 22 μg of $ZnSO_4 \cdot 7H_2O$, 10 μg of $CuSO_4 \cdot 5H_2O$, 10 μg of $CoCl_2 \cdot 6H_2O$, 6.3 μg of $Na_2MoO_4 \cdot 2H_2O$, 20 mg of $NaH_2PO_4 \cdot H_2O$, 100 μg of thiamine−HCl, 0.5 μg of biotin, and 0.5 μg of vitamin B12. For *D. parva*, 5 g of $MgCl_2$ and 4 g of Na_2SO_4 were added as well. The pH of the medium was adjusted to 6.0 before autoclaving, and a filter-sterilized solution of thiamine−HCl, biotin, vitamin B12, and $NaH_2PO_4 \cdot H_2O$ was added after autoclaving. Figure 9A shows the results from a 4-week culture of *D. parva*. The cell density was monitored daily by measuring spectrophotometrically the optical density (OD680) of the cell suspension from the bioreactors, using samples of cell suspensions of known cell concentration as standards. The pH and temperature of the culture medium were measured using the same samples. The temperature of the reactor surface and the greenhouse environment were monitored continuously. At days 6 and 12, a volume fraction of 30% of the cell suspension in the reactor was harvested and replenished with a fresh medium. The resulting cell densities are shown as the first two closed circles in Figure 9A. It is interesting to note that, after harvesting of the cells, 3 days of growth were required to reach the steady-state cell density. During the later stage of the culture, only 15% of the medium was harvested, and the cell density approached the steady-state level in 1 day. This improved the algal production and was continued for almost 2 weeks. It should be noted that during the first 2 weeks of operation the temperature control in the greenhouse was not installed. On a bright sunny day, the temperature inside the greenhouse was raised because the cooling capacity of the air conditioner was not sufficient to deal with the higher solar radiation input. The algae are darkly colored and thus absorb more radiation than the surrounding greenhouse, resulting in the higher reactor temperature as compared to the greenhouse.

Figure 9B presents the time course of an 8-week culture of *D. tertiolecta*. Here, the harvesting scheme was kept constant at 30% medium replacement. After the algae were adapted to the flue gas composition and environmental conditions, a 30% harvest per day was possible as shown in the second half of the culture. These results demonstrated that a continuous culture of algae using a flue gas is feasible.

The percent removal of CO_2 in the pilot installations was measured using a standard EPA testing procedure prescribed by the Code of Federal Regulations Title 40, Protection of Environment, Part 60, Appendix A, that applies to the determination of the CO_2 concentration from stationary sources. A continuous-emission measuring system was used that consisted of a thermoelectric water condenser (Baldwin), a flow controller for gas sample removal (CK Environmental), an infrared gas analyzer for CO_2 (California Analytical Instruments, model 3300), and a data chart recorder (Monarch, model 2000). The reduction level of CO_2 was measured continuously over a period of 7 days, as the difference between CO_2 concentrations at the bioreactor inlet and outlet, and expressed as a percent of the inlet CO_2 concentration. During sunny days (5 out of 7 days), the removal efficiency of CO_2 was $82.3 \pm 12.5\%$, and during cloudy days (2 out of 7), the removal efficiency of CO_2 was $50.1 \pm 6.5\%$. These removal efficiencies are significant and consistent with the photosynthetic metabolism of algae and the observed increases in algal biomass.

Summary

A particularly interesting application of ALRs is the growth of photosynthetic organisms because the fluid circulation can be utilized to provide the light−dark cycles necessary for photosynthesis. We focused on the flue gas treatment using algae for the absorption of CO_2 in a novel "triangular" ALR design. The effects of operating variables on the biomass production could be analyzed using a mathematical model of Wu and Merchuk[1] that accounted for the effects of the ALR geometry and fluid flow and the stimulatory and inhibitory effects of illumination on biomass growth. Testing of an array of ALRs operating with two different types of algae and continuously supplied with a flue gas from a small power plant demonstrated the feasibility of algal ALRs for the removal of CO_2 from flue gases. Further studies are underway to determine the ability of the system to remove NOx.

Acknowledgment

The design, fabrication, and operation of the laboratory- and pilot-plant systems described in this paper

would not be possible without the dedicated efforts of Javier de Luis, Joe Parrish, and Edison Guerra from Payload Systems Inc., Steve Drummey of George S. Drummey Co., and Peter Cooper and Roger Moore of MIT Utilities. The authors also thank Sue Kangiser for her expert help with manuscript preparation. Support for the project has been provided by GreenFuel Technologies Inc., Access Industries, Inc., NASA, and the Museum of Science, Boston.

Nomenclature

A_r = cross-sectional area of the riser [m^2]
A_d = cross-sectional area of the downcomer [m^2]
Dc = reactor diameter [m]
DX = volumetric yield [cells/cm^3·h]
G = gravitational constant [m/s^2]
J_G = superficial gas velocity [m/s]
H = draft tube height [m]
PFD = photon flux density [$\mu E/m^2$·s]
$I(\tau)$ = illuminance history of a photosynthetic cell [$\mu E/m^2$·s]
Pg = ground biomass yield [10^9 cell/m^2·h]
R = radial distance in the reactor [m]
T = time [s, days]
V = velocity [m/s]
X_1 = fraction of PSF in the open state
X_2 = fraction of PSF in the closed state
X_3 = fraction of PSF in the inhibited state
X = cell concentration [10^6 cells/cm^3]
x_f = final biomass concentration [kg/m^3]
α = kinetic constant for $x_1 \rightarrow x_2$ [$m^2/\mu E$]
β = kinetic constant for $x_2 \rightarrow x_3$ [$m^2/\mu E$]
γ = kinetic constant for $x_2 \rightarrow x_1$ [1/s]
k = kinetic constant for growth [$\mu E/m^2$·h]
μ = specific growth rate [1/h]
Me = maintenance term [1/h]

Subscripts

D = downcomer
r = riser
S = solid

Abbreviations

ALR = air-lift reactor
PFD = photon flux density
PSF = photosynthetic factory

Literature Cited

(1) Wu, X.; Merchuk, J. C. Simulation of Algae Growth in a Bench Scale Internal Loop Airlift Reactor. *Chem. Eng. Sci.* **2004**, *59* (14), 2899.

(2) Lazarova, V.; Meyniel, J.; Duval, L.; Menem, J. A. Novel Circulating Bed Reactor, Hydrodynamics, Mass Transfer and Nitrification Capacity. *Chem. Eng. Sci.* **1997**, *53*, 3919.

(3) Garcia-Calvo, E.; Rodriguez, A.; Prados, A.; Klein, J. A Fluid Dynamic Model for Three-Phase Airlift Reactors. *Chem. Eng. Sci.* **1999**, *54* (13−14), 2359.

(4) Freitas, C.; Fialova, M.; Zahradnik, J.; Teixeira, J. A. Hydrodynamic Model for Three-Phase Internal- and External-Loop Airlift Reactors. *Chem. Eng. Sci.* **1999**, *54* (21), 5253.

(5) Mousseau, F.; Liu, S. X.; Hermanowicz, S. W.; Lazarova, V.; Menem, J. Modeling of Turboflow−a Novel Reactor for Wastewater Treatment. *Water Sci. Technol.* **1998**, *37*, 177.

(6) Couvert, A.; Bastoul, D.; Roustan, M.; Line, A.; Chatellier, P. Prediction of Liquid Velocity and Gas Holdup in Rectangular Airlift Reactors of Different Scales. *Chem. Eng. Process.* **2001**, *40*, 113.

(7) Karamanev, D. G.; Nikolov, L. N. Application of Inverse Fluidization in Wastewater Treatment: From Laboratory to Full-Scale Bioreactors. *Environ. Prog.* **1996**, *15*, 194.

(8) Merchuk, J. C.; Shechter, R. Modeling of an Airlift Reactor with Floating Solids for Wastewater Treatment. *Can. J. Chem. Eng.* **2003**, *81* (3), 900.

(9) Radmer, R.; Behrens, P.; Fernandez, E.; Ollinger, O.; Howell, C. Algal Culture Studies Related to a Closed Ecological Life Support System. *Physiologist* **1984**, *27* (6, Suppl), S25.

(10) Merchuk, J. C. Shear Effects on Suspended Cells. *Adv. Biochem. Eng. Biotechnol.* **1991**, *44*, 65.

(11) Wu, X.; Merchuk, J. C. Measurement of Fluid Flow in the Downcomer of an Internal Loop Airlift Reactor Using an Optical Trajectory-Tracking System. *Chem. Eng. Sci.* **2003**, *58* (8), 1599.

(12) Kundakovic, L.; Vunjak-Novakovic, G. Mechanics of Particle Motion in Three-Phase Flow. *Chem. Eng. Sci.* **1995**, *50* (20), 3285.

(13) Barbosa, M. J.; Janssen, M.; Ham, N.; Tramper, J.; Wijffels, R. H. Microalgae Cultivation in Air-Lift Reactors: Modeling Biomass Yield and Growth Rate as a Function of Mixing Frequency. *Biotechnol. Bioeng.* **2003**, *82* (2), 170.

(14) Powles, S. B. Photoinhibition of Photosynthesis Induced by Visible Light. *Annu. Rev. Plant Physiol.* **1984**, *35*, 15.

(15) Krause, G. H. Photoinhibition of Photosynthesis. An Evaluation of Damaging and Protective Mechanism. *Physiol. Plant.* **1988**, *74* (566−574).

(16) Lee, Y. K.; Pirt, S. J. Energetics of Photosynthetic Algal Growth: Influence of Intermittent Illumination in Short (40 s) Cycles. *J. Gen. Microbiol.* **1981**, *124*, 43.

(17) Marra, J. Phytoplankton Photosynthetic Response to Vertical Movement in a Mixed Layer. *Mar. Biol. (Berlin)* **1978**, *46*, 203.

(18) Merchuk, J. C.; Ronen, M.; Giris, S.; Arad (Malis), S. Light/Dark Cycles in the Growth of the Red Microalga *Porphyridium* sp. *Biotechnol. Bioeng.* **1998**, *59*, 705.

(19) Eilers, P. H. C.; Peeters, J. C. H. A Model for the Relationship between Light Intensity and the Rate of Photosynthesis in Phytoplankton. *Ecol. Modell.* **1988**, *42* (3−4), 199.

(20) Wu, X.; Merchuk, J. C. A Model Integrating Fluid Dynamics in Photosynthesis and Photoinhibition Processes. *Chem. Eng. Sci.* **2001**, *56* (11), 3527.

(21) Wu, X.; Merchuk, J. C. Simulation of Algae Growth in a Bench Scale Bubble Column. *Biotechnol. Bioeng.* **2002**, *80*, 156.

(22) Merchuk, J. C.; Yunger, R. The Role of the Gas−Liquid Separator of Airlift Reactors in the Mixing Process. *Chem. Eng. Sci.* **1990**, *45* (9), 2973.

(23) Merchuk, J. C.; Ladwa, N.; Cameron, A.; Bulmer, M.; Pickett, A.; Berzin, I. Liquid Flow and Mixing in Concentric-Tube Airlift Reactors. *J. Chem. Technol. Biotechnol.* **1996**, *66*, 174.

(24) Barnea, D.; Shoham, O.; Taitel, Y. Flow Pattern Transition for Downward Inclined Two Phase Flow; Horizontal to Vertical. *Chem. Eng. Sci.* **1982**, *37* (5), 735.

(25) Barnea, D.; Shoam, O.; Taitel, Y.; Dukler, A. E. Flow Pattern Transition for Gas−Liquid Flow in Horizontal and Inclined Tubes. *Int. J. Multiphase Flow* **1980**, *6*, 217.

(26) Barnea, D.; Shoham, O.; Taitel, Y.; Dukler, A. E. Gas−Liquid Flow in Inclined Tubes: Flow Pattern Transitions for Upward Flow. *Chem. Eng. Sci.* **1985**, *40* (1), 131.

(27) Nagase, H.; Eguchi, K.; Yoshihara, K.-I.; Hirata, K.; Miyamoto, K. Improvement of Microalgal Nox Removal in Bubble Column and Airlift Reactor. *J. Ferment. Bioeng.* **1998**, *86*, 421.

(28) Heijnen, J. J.; Hols, J.; van der Lans, R. G. J. M.; van Leeuwen, H. L. J. M.; Mulder, A.; Weltevrede, R. A Simple Hydrodynamic Model for the Liquid Circulation Velocity in a Full-Scale Two- and Three-Phase Internal Airlift Reactor Operating in the Gas Recirculation Regime. *Chem. Eng. Sci.* **1997**, *52* (15), 2527.

(29) van Benthum, W. A. J.; van der Lans, R. G. J. M.; van Loosdrecht, M. C. M.; Heijnen, J. J. Bubble Recirculation Regimes in an Internal-Loop Airlift Reactor. *Chem. Eng. Sci.* **1999**, *54* (18), 3995.

(30) Hwang, S.-J.; Lu, W.-J. Gas−Liquid Mass Transfer in an Internal Loop Airlift Reactor with Low-Density Particles. *Chem. Eng. Sci.* **1997**, *52* (5), 853.

(31) Mudde, R. F.; Van Den Akker, H. E. A. 2d and 3d Simulations of an Internal Airlift Loop Reactor on the Basis of a Two-Fluid Model. *Chem. Eng. Sci.* **2001**, *56* (21−22), 6351.

(32) Camarasa, E.; Carvalho, E.; Meleiro, L. A. C.; Maciel Filho, R.; Domingues, A.; Wild, G.; Poncin, S.; Midoux, N.; Bouillard, J. A Hydrodynamic Model for Air-Lift Reactors. *Chem. Eng. Process.* **2001**, *40*, 121.

(33) Camarasa, E.; Carvalho, E.; Meleiro, L. A. C.; Maciel Filho, R.; Domingues, A.; Wild, G.; Poncin, S.; Midoux, N.; Bouillard, J. Development of a Complete Model for an Air-Lift Reactor. *Chem. Eng. Sci.* **2001**, *56* (2), 493.

(34) Sáez, A. E.; Márquez, M. A.; Roberts, G. W.; Carbonell, R. G. Hydrodynamic Model for Gas-Lift Reactors. *AIChE J.* **1998**, *44*, 1413.

(35) Márquez, M. A.; Sáez, A. E.; Carbonell, R. G.; Roberts, G. W. Coupling of Hydrodynamics and Chemical Reaction in Gas-Lift Reactors. *AIChE J.* **1999**, *45*, 410.

(36) Cockx, A.; Line, A.; Roustan, M.; Do-Quang, Z.; Lazarova, V. Numerical Simulation and Physical Modeling of the Hydrodynamics in an Air-Lift Internal Loop Reactor. *Chem. Eng. Sci.* **1997**, *52* (21−22), 3787.

(37) Tobajas, M.; Garcia-Calvo, E.; Siegel, M. H.; Apitz, S. E. Hydrodynamics and Mass Transfer Prediction in a Three-Phase Airlift Reactor for Marine Sediment Biotreatment. *Chem. Eng. Sci.* **1999**, *54* (21), 5347.

(38) Camacho Rubio, F.; Garcia, J. L.; Molina, E.; Chisti, Y. Axial Inhomogeneities in Steady-State Dissolved Oxygen in Airlift Bioreactors, Predictive Models. *Chem. Eng. J. (Lausanne)* **2001**, *84*, 43.

(39) Sanders, D. A.; Cawte, H.; Hudson, A. D. Modeling of the Fluid Dynamics Processes in a High-Recirculation Airlift Reactor. *Int. J. Energy Res.* **2001**, *25*, 487.

(40) Shechter, R.; Merchuk, J. C.; Ronen, T. Presented at WEFTEC, Chicago, IL, Sep 28−Oct 2, 2002 (unpublished).

(41) Orejas, J. A. Modelling and Simulation of a Bubble-Column Reactor with External Loop: Application to the Direct Chlorination of Ethylene. *Chem. Eng. Sci.* **1999**, *54* (21), 5299.

(42) Steiff, A.; Gran-Heedfeld, S.; Schlüter, S.; Weinspach, P. M. Presented at the Preprints of the 4th Japanese/German Symposium Bubble Columns, Kyoto, Japan, 1997 (unpublished).

Received for review September 15, 2004
Revised manuscript received May 9, 2005
Accepted May 18, 2005

IE049099Z